Tensile and Fatigue Behavior of Aluminum Oxide Fiber Reinforced Magnesium Composites: Part II. Alloying Effects

R. A. PAGE, J. E. HACK, R. SHERMAN, and G. R. LEVERANT

The effect of matrix alloy additions on mechanical properties was examined by comparing the tensile and fatigue properties of commercially pure magnesium and ZE41A (Mg-4.25 Zn-0.5 Zr-1.25 RE) which were both reinforced with FP aluminum oxide fibers. The alloy additions were found to improve the off-axis properties but decrease the axial properties. This was brought about by an increase in the matrix and interfacial strengths and a decrease in the fiber strength. It was also determined that the reaction zone in both materials was MgO and that strengthening of the interface was due to an increased particle size and/or a thicker reaction zone and not to any segregation of alloying elements to the interface.

I. INTRODUCTION

THE important effect that matrix composition and heat treatment have on off-axis properties has been demonstrated in a number of metal matrix composite systems.[1,2] Generally, these variables have not been found to influence axial properties. Although some attempts have been made to correlate matrix composition and heat treatment with corresponding changes in the toughness of the composite,[1] no quantitative correlations have been made with the local decohesion stress. In addition, effects of microstructural changes in the matrix have not been successfully separated from residual stress and interfacial effects.

A recent study (presented in Part I) of the fatigue and tensile behavior of a model material (FP Al_2O_3 fibers in a commercially pure Mg matrix) indicated that off-axis fatigue and tensile properties were suppressed because of the combination of a low fiber/matrix interfacial strength and a soft matrix. Under either cyclic or static loading the drastic drop in fatigue and tensile properties with angle was found to correspond with a change in failure mode from flat fracture across the fibers under axial loading conditions to interfacial and/or matrix failure along the fiber orientation for off-axis loading. One of the conclusions of the study was that alloy additions designed to increase the strength of the fiber/matrix interface and/or the strength of the matrix should improve off-axis properties. It has also been found that the transverse strength is dependent on matrix composition in FP/Mg composites.[3] It was not known whether this phenomenon was purely a matrix strengthening effect or due to a subtle change in interfacial structure.

This paper reports the initial results of a study of the influence of matrix composition on the micromechanisms of fracture and the tensile and fatigue properties of Al_2O_3 fiber reinforced magnesium composites. This work and earlier work on the model material (Part I) provide the foundation for a continuing program designed to develop quantitative relationships between matrix microstructure, composition, and properties; fiber orientation and volume percent; and fatigue crack growth behavior in these materials through direct observations of the effects of these variables on the strain field at the tip of a growing crack.

R. A. PAGE and J. E. HACK, Senior Research Metallurgists, R. SHERMAN, Research Metallurgist, and G. R. LEVERANT, Assistant Director, are all with the Department of Materials Sciences, Southwest Research Institute, 6220 Culebra Road, San Antonio, TX 78284.

Manuscript submitted September 8, 1983.

II. EXPERIMENTAL

The effect of matrix alloy content was investigated by comparing the fatigue and tensile properties of two materials which differed only in the composition of the matrix. Commercially pure magnesium (CPMg) was utilized as the baseline matrix material while ZE41A, a magnesium alloy with approximately 4.25 wt pct Zn, 0.5 wt pct Zr, and 1.25 wt pct rare earths, was chosen to represent alloyed matrix materials. Both materials contained 55 vol pct of continuous, unidirectional, 20 μm diameter Al_2O_3 fibers. The composite plates were manufactured by E. I. DuPont de Nemours and Co. by liquid infiltration of the FP Al_2O_3 fibers.

Specimens 15.2 cm long with 1.27 cm × 0.25 cm rectangular cross sections were used for both the tensile and fatigue tests. The specimens were machined with the Al_2O_3 fibers lying parallel to the 15.2 cm × 0.25 cm face and orientated at angles of 0, 22.5, 45, and 90 deg and 0 and 22.5 deg to the tensile axis for CPMg and ZE41A, respectively. Gripping was facilitated by the addition of aluminum tabs which were epoxied to both sides of the specimen ends.

A closed-loop hydraulic testing system was used for all of the mechanical tests. The fatigue tests were run under load control at an R-ratio of 0.1 and a frequency of 10 Hz. Samples were tested to failure or to approximately 10^6 cycles, whichever came first. The tensile tests were performed under displacement control at a strain rate of 8.3×10^{-5} per second. Specimen strain was determined from strain gages which were attached to opposite faces of the tensile specimens.

A. *Auger Spectroscopy*

To gain a better understanding of the effect of matrix composition on the fiber/matrix interface, transverse specimens of both CPMg and ZE41A were fractured *in situ* and examined in a Physical Electronics 595 scanning Auger microprobe. Surface spectra were taken with an incident accelerating voltage of 5 KeV and beam currents ranging from 0.3 μA to greater than 1 μA. Spectra were obtained in point mode, with a beam size of approximately

1 μm, and with the TV raster operating. All operating methods produced the same results within the chosen signal-to-noise conditions. A limited amount of ion sputtering was also performed.

B. *Transmission Electron Microscopy*

Thin foils of both composite materials were prepared by ion milling and examined in a Philips 301 scanning transmission electron microscope. Microdiffraction patterns were obtained by limiting the specimen area illuminated with a focused second condenser aperture.[4] A 5 μm aperture was used which, with the demagnification of 38 times obtained in the Philips 301 STEM, yielded an illuminated area of approximately 130 nm in diameter. Diffraction patterns were taken at multiple orientations so that the interface particles could be unambiguously identified.

III. RESULTS

A. *Tensile Behavior*

It is clear from the tensile data, Table I and Figure 1, that the alloy additions to the matrix had a strong influence on both the yield, *YS*, and ultimate tensile, *UTS*, strengths. Under axial loading, the use of ZE41A as a matrix material rather than CPMg resulted in approximately a 50 pct increase in *YS* and a 15 pct decrease in *UTS*. At 22.5 deg the ZE41A material demonstrated increased *YS* and *UTS* with the *UTS* increased by about a factor of two and the *YS* by an order of magnitude over the CPMg material. As expected, the elastic modulus at 0 and 22.5 deg was not significantly affected by the alloy additions. Thus, the alloy additions in ZE41A, *i.e.*, Zn, Zr, and rare earths, benefited the off-axis tensile properties and the axial yield strength but reduced the axial *UTS*.

The fracture morphology of the axial specimens was found to be independent of the matrix composition. Both the CPMg and the ZE41A axial specimens failed in a flat manner at approximately 90 deg to the stress axis with the failure propagating across fibers. The off-axis behavior was highly composition dependent, however. Failure of the 22.5 deg ZE41A specimens was similar to that of the axial specimens. The fracture surface was quite flat, oriented at 90 deg to the tensile axis, and fracture occurred through the fibers. In direct contrast, the off-axis CPMg specimens failed along the fiber/matrix interface.

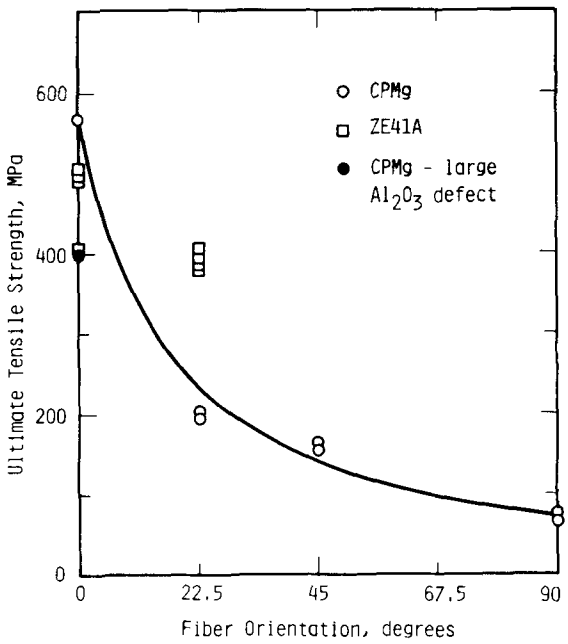

Fig. 1—Effect of fiber orientation on ultimate tensile strength for both commercially pure magnesium and ZE41A matrix materials.

B. *Fatigue Behavior*

The results of fatigue tests performed on CPMg and ZE41A in both 0 and 22.5 deg orientations are presented in Figure 2. When loaded axially the fatigue resistance of ZE41A was considerably lower than that of CPMg. However, although both materials showed a marked reduction in fatigue resistance when loaded off-axis (22.5 deg), the degree of reduction was far less for ZE41A than for CPMg. Thus, at 22.5 deg ZE41A was more resistant to fatigue than CPMg. This behavior is similar to the *UTS* dependence on alloy content and fiber orientation. The S-N curves for ZE41A exhibited slightly steeper slopes than the corresponding curves for CPMg. Thus, the endurance limit, 10^6 cycles to failure, for ZE41A was approximately 0.62 *UTS* for both 0 deg and 22.5 deg while CPMg had an endurance

Table I. Mechanical Properties of 55 Vol Pct Al_2O_3 Fiber Reinforced Magnesium

Specimen	Matrix Material	Orientation, Degrees	*YS*, MPa	*UTS*, MPa	*E*, GPa
CP-O-A	CPMg	0		399*	192
CP-O-B	CPMg	0	321	567	202
CP-22-A	CPMg	22.5	30	192	153
CP-22-B	CPMg	22.5	23	199	157
ZE-O-A	ZE41A	0	—	488	186
ZE-O-B	ZE41A	0	—	504	184
ZE-O-C	ZE41A	0	487	496	—
ZE-O-D	ZE41A	0	406	406	—
ZE-22-A	ZE41A	22.5	—	393	157
ZE-22-B	ZE41A	22.5	—	379	155
ZE-22-C	ZE41A	22.5	325	406	—
ZE-22-D	ZE41A	22.5	325	388	—

*The *UTS* of specimen CP-O-A was reduced well below typical values by the presence of an unusually large process defect. This is discussed more fully in Part I.

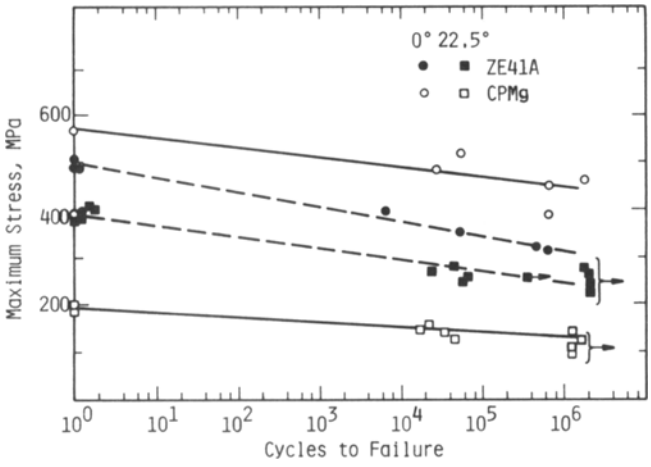

Fig. 2 — Effect of fiber orientation and matrix alloy addition on the fatigue behavior of Al_2O_3 fiber-reinforced magnesium.

limit of approximately 0.68 *UTS* at 22.5 deg and 0.78 *UTS* at 0 deg.

The axial CPMg and ZE41A specimens exhibited similar fracture morphologies. In both, fracture occurred across the fibers at an angle of approximately 90 deg to the tensile axis. The fracture morphology of the off-axis specimens was affected by the matrix composition, however. The 22.5 deg CPMg specimens failed parallel to the fiber axis with a significant difference between the fatigue and overload morphologies. The overload regions, Figure 3(a), failed by decohesion of the fiber/matrix interface while fatigue cracking (Figure 3(b)) occurred along the direction of the fiber axis by a combination of crystallographic matrix cracking and delamination of the fiber/matrix interface. The 22.5 deg ZE41A specimens, on the other hand, failed across the fibers at around 90 deg to the tensile axis in both fatigue and overload (Figure 4) in the same manner as the axial specimens.

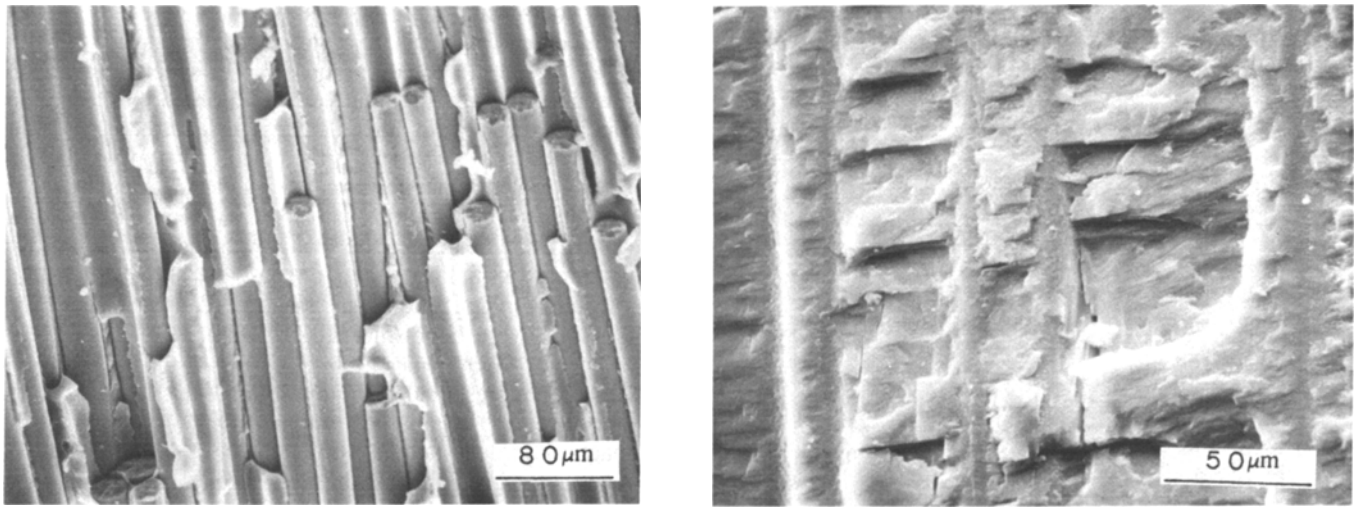

(*a*) (*b*)

Fig. 3 — Scanning electron micrographs of typical overload (*a*) and fatigue (*b*) failures in off-axis CPMg specimens. Note that the failure in overload occurs almost exclusively along fiber/matrix interfaces while subcritical fatigue crack growth occurs parallel to the interfaces but primarily through the matrix.

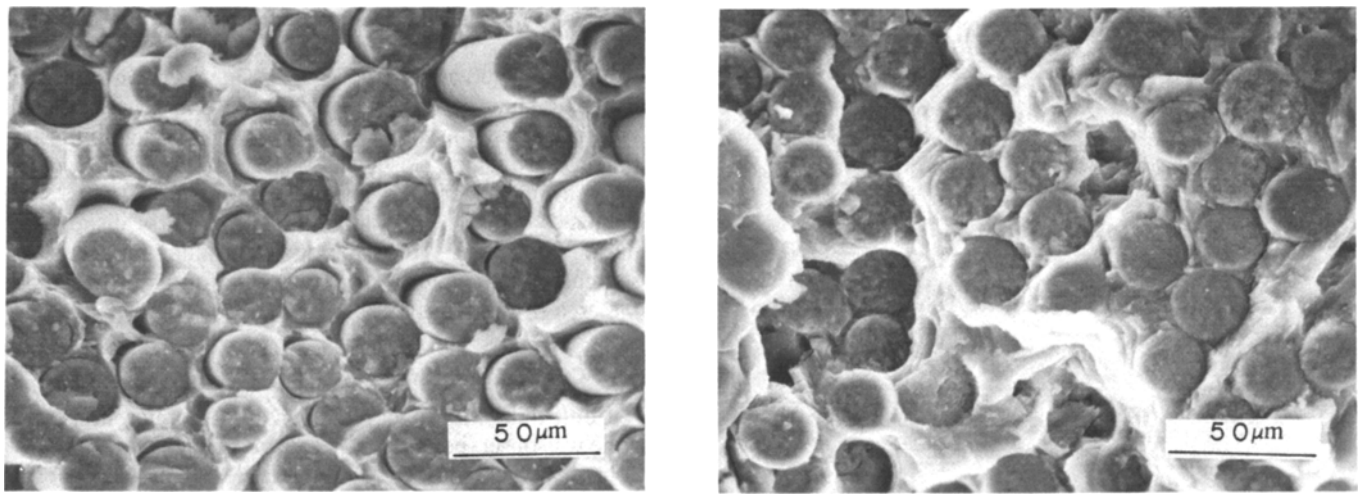

(*a*) (*b*)

Fig. 4 — Scanning electron micrographs illustrating typical fracture morphology (*a*) far from the initiation site, considered the overload region, and (*b*) adjacent to the initiation site, considered the fatigue region in off-axis ZE41A specimens. Although there is more evidence of ductile tearing in the overload region, failure in both regions occurs across the fibers rather than along or parallel to the fiber/matrix interface.

The similarity in the appearance of the fatigue and overload regions of the 0 deg and 22.5 deg ZE41A specimens and the 0 deg CPMg specimens made it impossible to determine the extent of fatigue cracking. River markings on the fracture surface did identify fatigue crack initiation sites, however. In both CPMg and ZE41A fatigue cracks initiated at process defects, usually large clumps of Al_2O_3 grains. These defects were not involved in initiation in the 22.5 deg CPMg specimens. Examination of mating fracture surfaces in CPMg specimens indicated that failure occurred along the defect/matrix interface. Energy dispersive X-ray spectra taken from the mating surfaces always showed aluminum (Al_2O_3) on one surface and primarily magnesium on the other, confirming that fracture was along the interface. The mating fracture surfaces in ZE41A indicated that failure occurred through the defect rather than along its interface. Thus, although the initiation sites were similar, the failure modes of the defects changed with matrix composition.

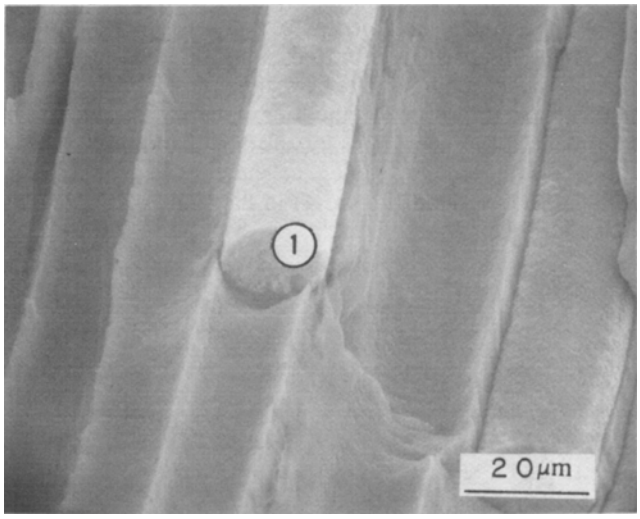

(*a*)

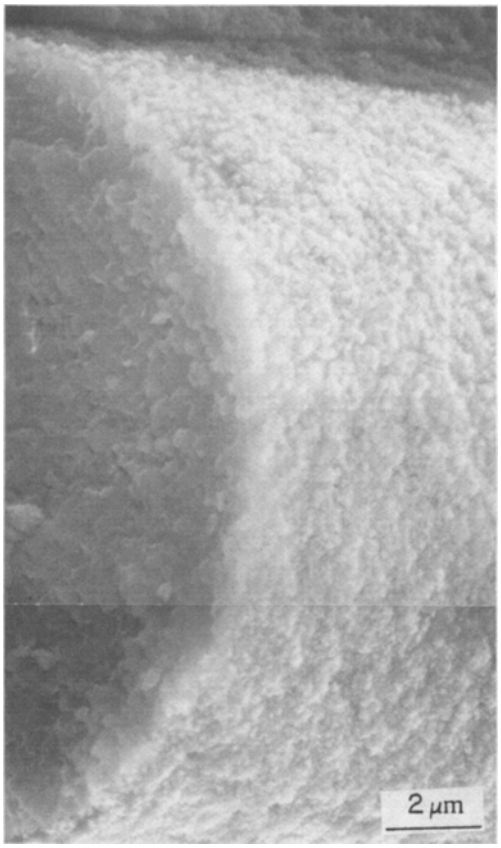

(*b*)

Fig. 5 — Scanning electron micrographs of a CPMg specimen fractured in the scanning Auger microprobe. A high magnification view of the fiber surface in Area 1 is shown in (*b*).

C. *Auger Spectroscopy*

The *in-situ* fracture of both CPMg and ZE41A occurred along fiber/matrix interfaces, making it possible to examine the composition of both troughs and fiber surfaces. Microscopic examination of the fiber surfaces in the Scanning Auger microprobe indicated that the fibers in CPMg (Figure 5) were covered with fine, almost continuous particles while the fibers in ZE41A (Figure 6) were covered with coarser and more discrete particles.

Spectra taken from a fiber trough and the surface of a fiber in CPMg are presented in Figure 7. The spectra indicate the presence of magnesium and oxygen in both the trough and the fiber surface. No other elements were observed on either the trough or the fiber surface. Comparison of the fine structure of the magnesium peaks and the oxygen-to-magnesium peak height ratios with spectra taken from laboratory standards[5] indicates that the trough was metallic magnesium containing a small amount of oxygen, possibly from residual vacuum contamination, and that the fiber surface was an oxide of magnesium, most likely MgO.

Spectra from a fiber trough and the surface of a fiber in ZE41A are presented in Figure 8. As in the CPMg, the fine structure of the magnesium peaks and the oxygen-to-magnesium peak height ratios indicate that the trough was metallic magnesium and the fiber surface was an oxide of magnesium. In addition to the magnesium and oxygen, small quantities of zinc and aluminum were also present in both locations. No evidence of the presence of zirconium or rare earths, the other alloying elements in ZE41A, was found on either the trough or the fiber surface. The small carbon peak observed in the trough spectra is probably due to contamination rather than the actual presence of carbon in the specimen. To determine if either the zinc or aluminum were segregated at the fiber/matrix interface ion sputtering of the fracture surface was performed. No decrease in the zinc or aluminum signals was observed during sputtering; rather, a slight increase was observed (Figure 8(b)). The oxygen peak decreased and the carbon peak, which was believed to be due to contamination, quickly disappeared during sputtering. Thus, the zinc and aluminum were not segregated at the interface but rather uniformly distributed in the area of the interface.

D. *Transmission Electron Microscopy*

Confirming the Auger results, a thin, submicron, reaction zone was observed in the thin foils of both CPMg (Figure 9) and ZE41A (Figure 10). The reaction zone particles in CPMg were finer, 0.14 μm average diameter *vs* 0.24 μm average diameter in ZE41A, and more closely spaced than those in ZE41A, thus presenting a geometrically smoother matrix/reaction zone interface. In addition, the reaction

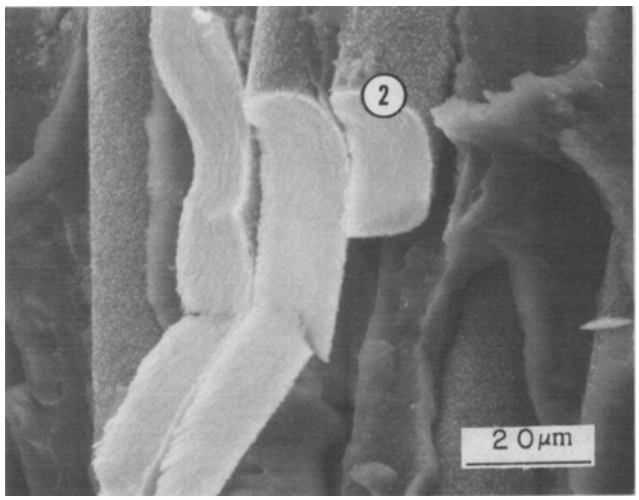

(*a*)

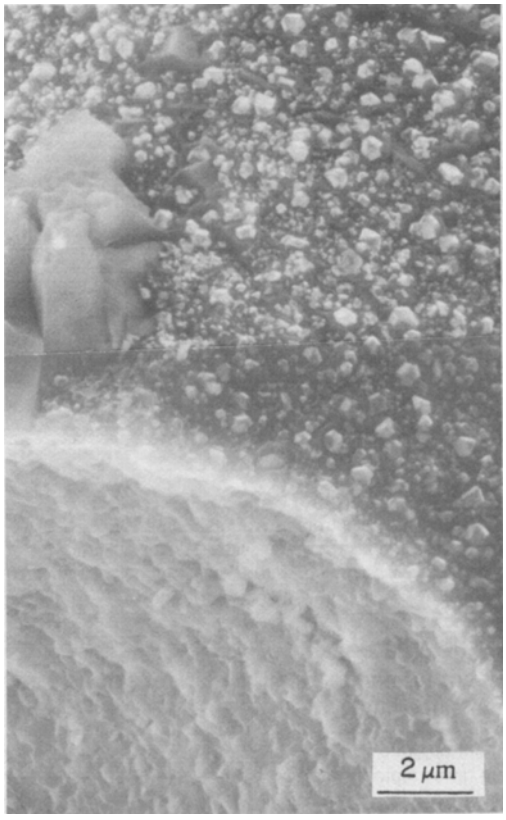

(*b*)

Fig. 6 — Scanning electron micrographs of a ZE41A specimen fractured in the scanning Auger microprobe. A high magnification view of the fiber surface in Area 2 is shown in (*b*).

zone in CPMg was approximately a factor of two thinner than the 0.2 μm thick reaction zone in ZE41A. A considerable variation in grain size was also observed in the Al_2O_3 fibers.

The reaction zone precipitates were identified as MgO by microdiffraction. Typical microdiffraction patterns, (110) zone axis, are presented in Figures 9 and 10. In both CPMg and ZE41A the particles were cubic with lattice parameters of 0.4230 and 0.4210 nm, respectively. These values are within measurement error of the published MgO lattice parameter of 0.4213 nm.[6]

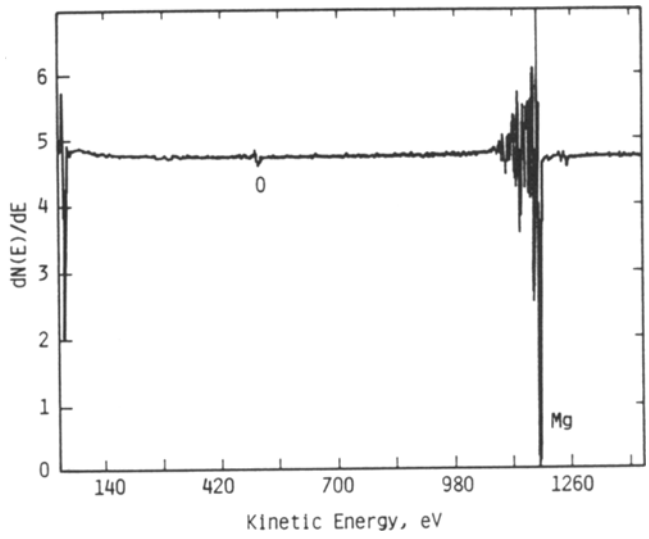

(*a*)

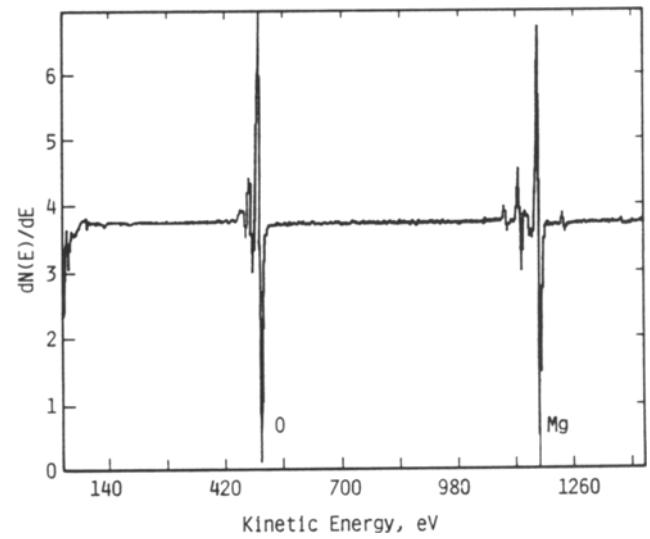

(*b*)

Fig. 7 — Auger electron spectra taken from the fiber trough (*a*) and the fiber surface (*b*) of a CPMg sample which was fractured *in situ*.

IV. DISCUSSION

The properties of a composite material are determined by a combination of the fiber, matrix, and interfacial properties. In general, axial strength, both static and cyclic, is primarily dependent on the fiber volume fraction and the fiber strength. Matrix strength plays only a secondary role. On the other hand, transverse strength is more heavily influenced by the matrix and interfacial strengths. At intermediate angles the component controlling failure is controlled by the relative magnitudes of the shear and normal stresses that each component experiences as well as the individual strengths of each component. In general, matrix alloy additions can affect all three of the parameters that control composite behavior, *i.e.*, fiber, matrix, and interfacial properties.

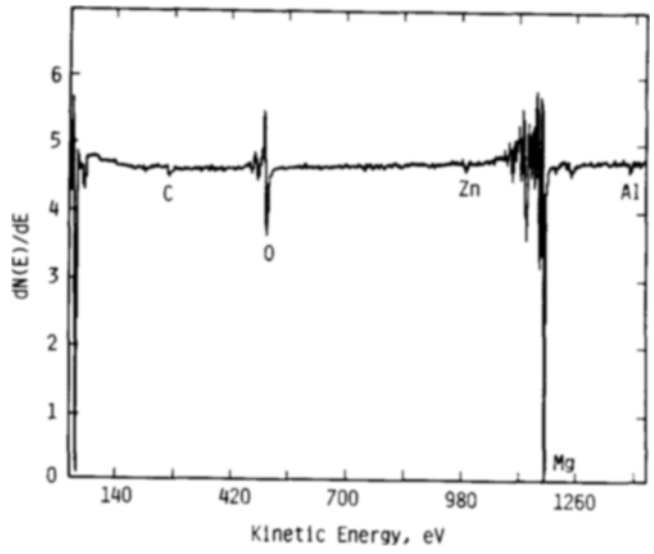

(*a*)

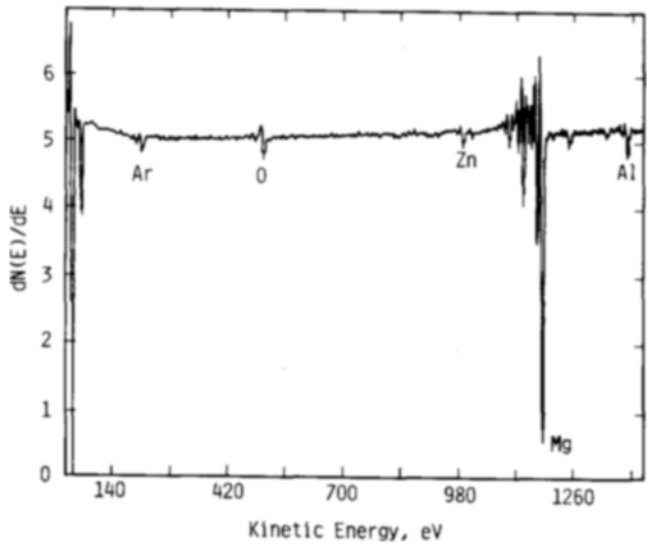

(*b*)

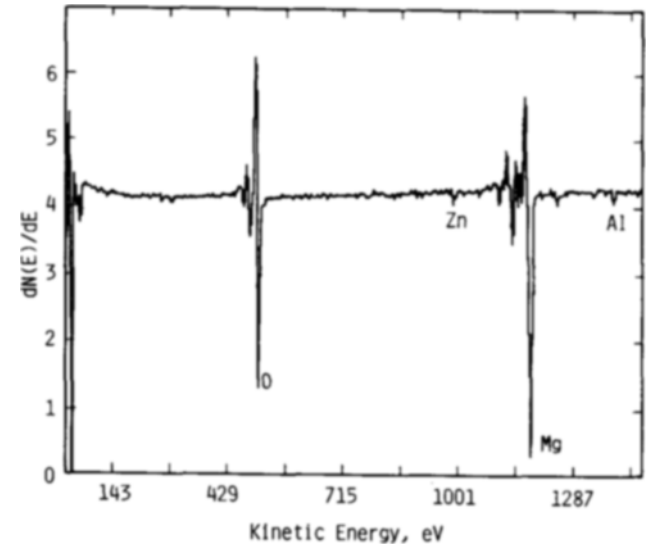

(*c*)

Fig. 8 — Auger electron spectra taken from the fiber trough before (*a*) and after (*b*) sputtering and from the fiber surface (*c*) of a ZE41A sample which was fractured *in situ*.

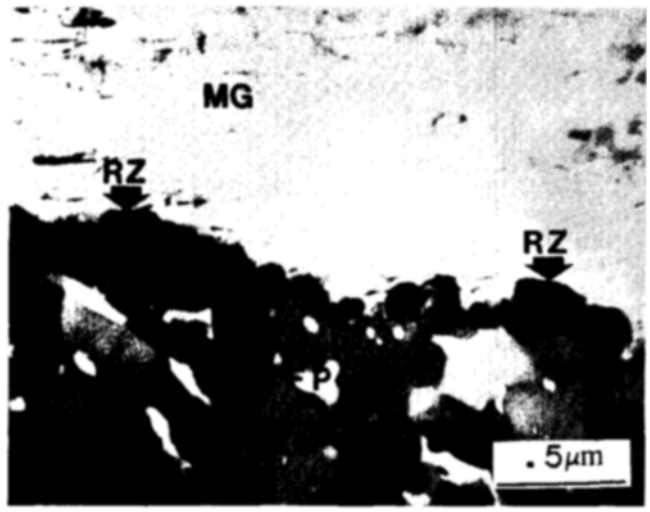

(*a*)

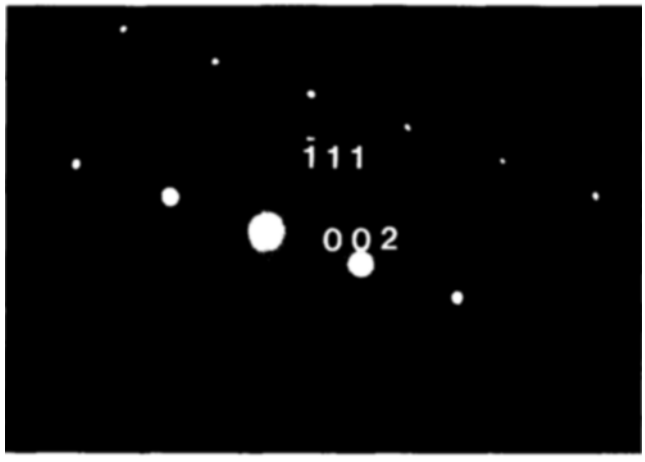

(*b*)

Fig. 9 — Transmission electron micrograph of the fiber/matrix reaction zone in CPMg (*a*) and a diffraction pattern taken from a typical reaction zone particle (110 Zone) (*b*). The various constituents are indicated by: MG (CPMg matrix); RZ (reaction zone product); and FP (Al_2O_3 fiber).

Although the microstructural state of the ZE41A matrix material is uncertain,* it is still possible to discuss, in terms of upper and lower limits, the effect of the alloy additions on matrix strength. In the fully solutionized condition substantial solid solution strengthening would be provided by the zinc. This lower limit case would provide a considerable improvement in matrix strength compared to CPMg. The zinc additions can also lead to precipitation hardening through the formation of Guinier-Preston zones, MgZn′ precipitates, or MgZn precipitates.[7,8] The formation of Mg_7Zn_3 is also possible.[9] The presence of any of these precipitates would further strengthen the matrix. The presence of zirconium, which acts as a grain refiner in magnesium castings, is probably responsible for the slightly smaller grain size of the ZE41A. However, since the grain sizes of ZE41A and CPMg were both much larger than the fiber spacing, it

*It was not possible to define the microstructural state because data on the cooling rates employed during casting were not available. Further, the ion milling procedure employed in foil preparation could heat the foils slightly, thus altering the matrix precipitate morphology.

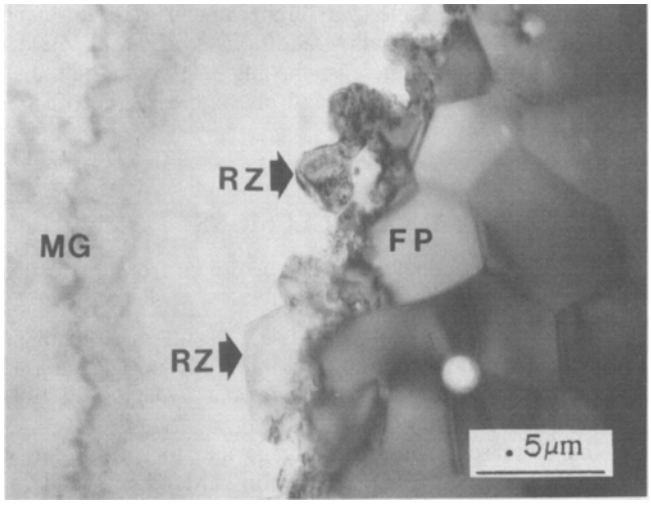

(*a*)

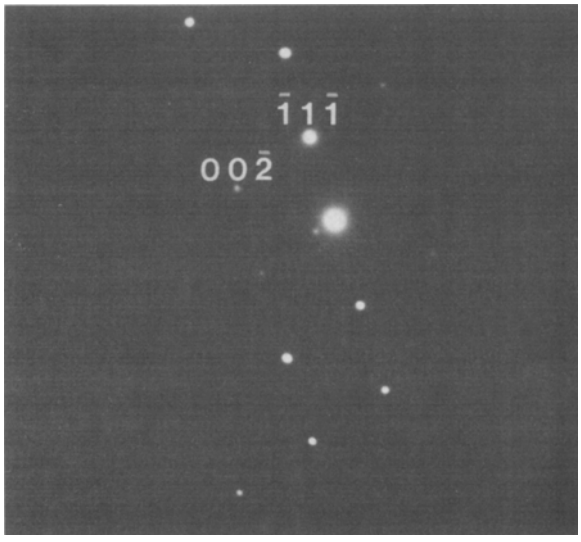

(*b*)

Fig. 10—Transmission electron micrograph of the fiber/matrix reaction zone in ZE41A (*a*) and a diffraction pattern taken from a typical reaction zone particle (110 Zone) (*b*). The various constituents are indicated by: MG (ZE41A matrix); RZ (reaction zone product); and FP (Al_2O_3 fiber).

is doubtful that grain size has any significant bearing on mechanical properties. One might expect, therefore, that use of ZE41A rather than CPMg would result in a matrix with a higher yield strength, ultimate tensile strength, and fatigue resistance.

Since ZE41A has a higher matrix strength than CPMg, the lower axial tensile strength of the ZE41A material indicates that the fiber strength of the ZE41A is degraded. Using the rule of mixtures and a *UTS* of 90 MPa for the CPMg matrix, the resultant strength of the Al_2O_3 fibers is 950 MPa. A similar calculation for ZE41A using 165 MPa as the matrix strength[10] yields a fiber strength of 770 MPa. This represents a 19 pct reduction in fiber strength. Since the same type of fiber, *i.e.*, FP Al_2O_3, was used in both materials and the CPMg fiber strength of 950 MPa is near the bottom of the scatter band,[11] it can be concluded that the reduced fiber strength of ZE41A is due to reaction with the matrix material.

The crossover of the *UTS vs* fiber orientation curves suggests that the matrix and/or interfacial strength of ZE41A is higher than CPMg. From the earlier discussion of the effect of alloy additions on matrix strength, it is obvious that the ZE41A material has a higher matrix strength than the CPMg material. The change in off-axis fracture morphology from interfacial failure in CPMg to flat fracture across fibers in ZE41A suggests that the ZE41A material also has a higher interfacial strength. The change in the fracture mode of the process defects which act as fracture initiation sites from interfacial failure in CPMg to fracture through the defect in ZE41A also supports an increased interfacial strength in ZE41A.

The reaction product was identified as MgO in both materials by microdiffraction. The TEM observations also indicated that the reaction zone in ZE41A was thicker and made up of larger particles than in CPMg. Thermodynamic calculations indicate that the formation of MgO from Al_2O_3 and Mg is possible for matrix magnesium concentrations exceeding 4 to 8 pct,[12] a condition which both CPMg and ZE41A easily satisfy. Further, Levi *et al.*[12] have observed the formation of both MgO and $MgAl_2O_4$ spinel on FP Al_2O_3 fibers in contact with an Al-8 pct Mg alloy. The formation of MgO has also been observed in Al_2O_3 scales on Al-Mg alloys.[13] The above results and the findings of the present study disagree with an earlier identification of the FP AL_2O_3/ZE41A reaction product as $MgAl_2O_4$,[14] which was performed by X-ray analysis of bulk specimens. Although the presence of $MgAl_2O_4$ is apparent from the X-ray data, the use of bulk specimens in the study precludes any identification of its location. Energy dispersive X-ray analysis profiles taken across the fiber/matrix interface[14] are also inconclusive as to the nature of the reaction product since the spacial resolution of the analysis was larger than the 0.2 μm reaction zone which is present in this material. The Auger results support the formation of MgO in the reaction zone and, further, indicate that interfacial failure in both materials occurs at the reaction zone/matrix interface as opposed to the reaction zone/fiber interface. In addition, the lack of any segregation at the reaction zone/matrix interface indicates that the alloying elements in ZE41A were not directly responsible for the increased interfacial strength. Hence, it can be concluded that the interfacial strengthening observed in ZE41A is due to an increase in the size of the reaction zone and/or a change in the size and spacing of the MgO crystals and not any change in the chemical nature of the reaction zone. The increased reaction zone is also consistent with the degradation in fiber strength observed in ZE41A. A large fraction of the reduced fiber strength is believed to be due to the development of notches on the fiber surfaces, induced by uneven chemical attack on the fibers during precipitation and growth of the MgO particles, since the actual reduction in Al_2O_3 cross section brought about by the formation of MgO accounts only for a small portion of the observed reduction. This explanation is consistent with observations in other composite systems.[15,16,17]

The TEM and Auger results indicate that the matrix alloying elements are not incorporated in the reaction zone to any significant degree. Hence, the only plausible explanation for the differences observed in the sizes of the reaction zones between CPMg and ZE41A would be an inherent difference

in processing. Liquidus temperatures, liquid metal infiltration temperatures, and cooling rates were similar for the two alloys.[18,19] A major difference exists in the solidification behavior, however. CPMg should undergo nearly congruent solidification while ZE41A experiences a large "mushy" zone due to the 120 °C difference between its liquidus and solidus temperatures.[18] It is postulated, therefore, that the larger reaction zone in ZE41A results from a longer contact time with more highly reactive liquid matrix. Experiments to test this hypothesis are presently underway.

To summarize the discussion to this point, the matrix alloy additions result directly in an increased matrix strength and indirectly in an increased interfacial strength and a decreased fiber strength. These results, which are consistent with the differences in tensile behavior between CPMg and ZE41A, can also be used to explain the differences in fatigue behavior between the two materials. Under axial loading the fibers bear most of the load and present the primary barrier to fatigue. Thus, the reduction in fiber strength through an increased reaction zone observed in ZE41A would be expected to yield reduced fatigue resistance. The lower interfacial strength in CPMg may also contribute to CPMg's higher fatigue resistance.[20]

For one to understand the differences in off-axis fatigue behavior between CPMg and ZE41A it is necessary to consider both the strength differences of the individual components and the mechanics involved in off-axis loading. For loading at 22.5 deg to the fiber matrix, the off-axis orientation employed in this study, a relatively high normal stress and a relatively low shear stress would exist in the fibers, while a crack propagating along the fiber direction either in the matrix or along the interface would experience a relatively low normal stress and a relatively high shear stress.[21] Considering this and the earlier observation that fatigue crack propagation in CPMg oriented at 22.5 deg occurred by a combination of crystallographic cracking of the Mg matrix and interfacial failure, it can be concluded that failure of the matrix-interface combination is possible at lower applied stresses than is normal fracture of the fibers.

Although the ZE41A matrix is also susceptible to the same type of crystallographic cracking as the CPMg matrix,[9,22] its fatigue resistance is substantially higher. In addition, the ZE41A composite has a higher interfacial strength, the other component which contributed to fatigue crack propagation in CPMg; and a lower fiber strength, the component which did not participate in failure in CPMg. By increasing the fatigue resistance of the two weaker components and, at the same time, decreasing the resistance of the strongest component, a point should be reached at which a transition in fracture mode to progressive fracture of fibers occurs. This is apparently what has taken place in the ZE41A material.

The fracture and fatigue behavior of ZE41A at misorientation angles greater than 22.5 deg can be postulated by once again considering the mechanics of off-axis loading. As the misorientation angle increases, the fibers experience lower normal stresses and cracks oriented along the fiber direction, *i.e.*, either matrix or interfacial cracks, experience higher normal stresses.[21] Thus, at some higher angle, a transition to matrix and/or interfacial failure along the fiber direction would be expected. Even so, the ZE41A material would still be expected to maintain a higher strength than CPMg due to its higher matrix and interfacial strengths. Hence, the alloy additions present in ZE41A would be expected to increase the angle at which the transition in failure mode occurs and also increase the off-axis strength.

V. CONCLUSIONS

The following conclusions can be drawn from the results of the present investigation:

1. The alloying elements in ZE41A result directly in an increased matrix strength and indirectly in an increased fiber/matrix interfacial strength and a decreased fiber strength when compared to CPMg.
2. The increased matrix strength is due to solid solution strengthening and/or precipitation hardening.
3. The increased interfacial strength is due to a larger reaction zone and larger particles and not to any segregation to or change in chemistry of the reaction zone. The reaction zone was made up of MgO in both CPMg and ZE41A and interfacial failure occurred along the reaction zone/matrix interface. Segregation to this interface was not observed.
4. The decreased fiber strength, which was estimated to be approximately 20 pct, was the result of the increased reaction between the matrix and fibers.
5. The changes in the component strengths for ZE41A outlined above yielded reduced axial and increased off-axis tensile and fatigue properties.

ACKNOWLEDGMENTS

The authors are grateful for the support of this work by the Army Research Office under Contract No. DAAG29-81-K-0049. The assistance in thin foil preparation which Mr. H. G. Saldana provided is also gratefully acknowledged.

REFERENCES

1. W. R. Hoover: *J. Comp. Mat.*, 1976, vol. 10, p. 106.
2. K. M. Prewo and K. G. Kreider: *J. Comp. Mat.*, 1972, vol. 6, p. 338.
3. W. R. Kreuger: E. I. DuPont de Nemours and Co., Wilmington, DE, private communication, September 1979.
4. W. D. Riecke: *Optik*, 1962, vol. 19, p. 81.
5. L. E. Davis, N. C. MacDonald, P. W. Palmberg, G. E. Riach, and R. E. Weber: *Handbook of Auger Electron Spectroscopy*, 2nd ed., Physical Electronic Industries, Eden Prairie, MN, 1976, pp. 39-41.
6. *X-Ray Powder Data File*, ASTM STP 48-J, J. V. Smith, ed., American Society for Testing Materials, Philadelphia, PA, 1960, p. 581.
7. J. B. Clark: *Acta Metall.*, 1965, vol. 13, p. 1281.
8. G. Mima and Y. Tanaka: *Jap. Inst. Met.*, 1971, vol. 12, p. 71.
9. A. K. Bhambra and T. Z. Kattamis: *Metall. Trans.*, 1971, vol. 2, p. 1869.
10. J. Nunes: Report No. AMMRC SP 83-3, Army Materials and Mechanics Research Center, Watertown, MA, April 1983.
11. R. T. Pepper and D. C. Nelson: Report No. NASA CR-167999, NASA-Lewis Research Center, Cleveland, OH, September 1982.
12. C. G. Levi, G. J. Abbaschian, and R. Mehrabian: *Metall. Trans. A*, 1978, vol. 9A, p. 697.
13. A. J. Brock and M. A. Heine: *J. Electrochem. Soc.*, 1972, vol. 119, p. 1124.
14. E. Chin: Report No. AMMRC SP 83-3, Army Materials and Mechanics Research Center, Watertown, MA, April 1983.

15. D. W. Petrasek and J. W. Weeton: *Trans. TMS-AIME*, 1964, vol. 230, p. 977.
16. A. G. Metcalfe: *J. Compos. Mater.*, 1967, vol. 1, p. 356.
17. A. Pattnaik and A. Lawley: *Metall. Trans.*, 1974, vol. 5, p. 111.
18. *ASM Metals Handbook, 9th ed., Volume 2—Properties and Selection: Nonferrous Alloys and Pure Metals*, ASM, 1979, p. 523.
19. J. Widrig: E. I. DuPont de Nemours and Co., Wilmington, DE, private communication, October 1983.
20. M. Gouda, K. M. Prewo, and A. J. McEvily: *Fatigue of Fibrous Composite Materials*, ASTM STP 723, K. N. Lauraitis, ed., American Society for Testing Materials, Philadelphia, PA, 1981, pp. 101-15.
21. C. C. Chamis and J. H. Sinclair: Report No. NASA TN D-8215, NASA-Lewis Research Center, Cleveland, OH, April 1976.
22. M. J. May and R. W. K. Honeycombe: *J. Inst. Metals*, 1963-64, vol. 92, p. 41.